

Self-heating ignition of open-circuit cylindrical Li-ion battery pile: Towards fire-safe storage and transport

Yanhui Liu^a, Peiyi Sun^a, Shaorun Lin^a, Huichang Niu^{b,*}, Xinyan Huang^{a,*}

^a*Department of Building Services Engineering, The Hong Kong Polytechnic University, Hong Kong*

^b*Institute of Industry Technology, Guangzhou & Chinese Academy of Sciences, China*

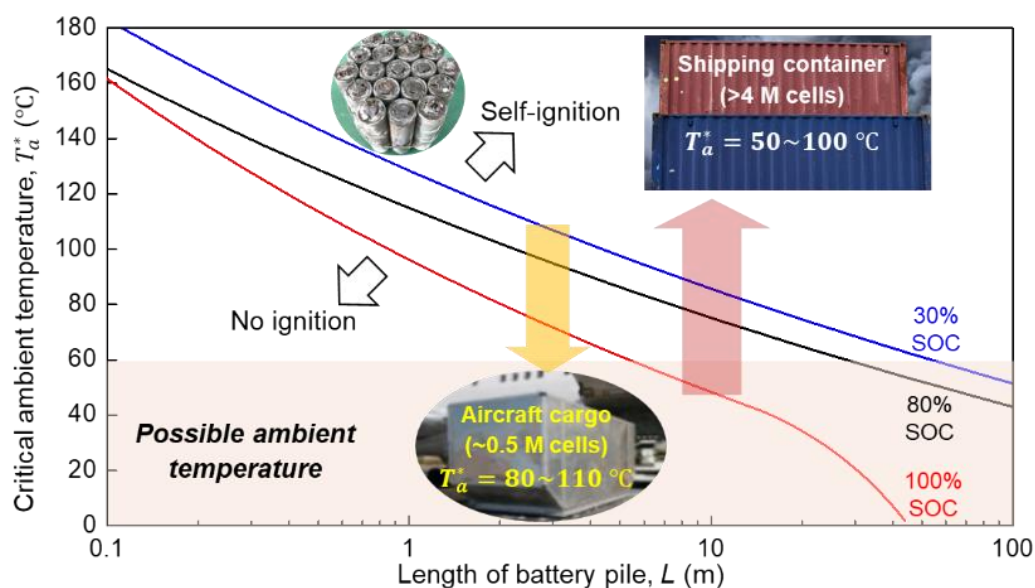
*Corresponding to xy.hang@polyu.edu.hk (X. Huang)

Abstract

The battery fire accidents frequently occur during the storage and transportation of massive Lithium-ion batteries, posing a severe threat to the energy-storage system and public safety. This work experimentally investigated the self-heating ignition of open-circuit 18650 cylindrical battery piles with the state of charge (SOC) from 30% to 100% and the cell number up to 19. As the ambient temperature increases, the self-heating ignition occurs and leads to a violent fire. The characteristic temperatures for both electrolyte leaking and thermal runaway decrease with SOC. The critical ambient temperature for self-heating ignition ranges from 135 °C to 192 °C, and it decreases with the increasing battery SOC, cell number, and pile size, which satisfies the self-ignition theory. The applied Frank-Kamenetskii analysis predicts the self-ignition ambient temperature could be lower to 30 °C for large battery piles with multiple tightly packed layers, such as those in the shipping container and warehouse. Nevertheless, creating gaps and providing effective cooling between each battery layer could effectively lower the fire risk by increasing the self-ignition ambient temperature above 125 °C. This work theoretically reveals the self-ignition characteristics of open-circuit battery piles, which could provide scientific guidelines to improve battery safety and reduce fire hazards during storage and transportation.

Keywords: Lithium-ion battery safety; thermal runaway; self-ignition; critical size

Graphic Abstract



Nomenclature

Symbols		N	number of battery cells (-)
D	battery pile diameter (m)	R	universal gas constant (J/mol-K)
E	activation energy (kJ/mol)	SOC	state of charge (%)
f	mass function (g/m ³ -s)	T	temperature (K)
$F-K$	Frank-Kamenetskii	T_a^*	critical self-ignition ambient temperature (K)
H	battery height (m)		
ΔH	heat of reactions (kJ/kg)	Greeks	
k	thermal conductivity (W/m-K)	δ_{cr}	Frank-Kamenetskii number (-)
L	characteristic length (m)		
$Li-ion$	Lithium-ion	Subscripts	
m	mass (g)	a	ambient
Δm	mass loss (g)	b	battery

1. Introduction

The Lithium ion (Li-ion) battery has been widely used in most of the portable electric devices, electric vehicles, and energy storage systems because of their extremely high-power density [1–3]. In practice, a large quantify of Li-ion batteries are tightly packed to save storage space and improve transportation efficiency. Although Li-ion batteries are categorized as class 9 dangerous goods by the United Nations and have to meet the mandatory test criteria for transport [4], numerous catastrophic battery fire accidents have still occurred during storage and transportation. For instance, in 2013, a Li-ion battery pack in a Boeing 787 caught fire when the plane landed for maintenance at Boston’s Logan International Airport (Fig. 1a). Recently, along with the increase in Li-ion battery production and international trade, battery fires in storage and transport become more frequent (Fig. 1b-d).



Fig. 1. (a) A Li-ion battery pack in a Boeing 787 caught fire at Boston’s Logan International Airport in 2013 [26]; (b) an aviation container carrying Li-ion batteries caught fire at Hong Kong International Airport in 2019 [27]; (c) the battery fire occurred in a warehouse in 2019 [28]; and (d) Li-ion batteries caught fire in the containers of China Ocean Shipping Company in 2020 [29,30].

These fire accidents led to many casualties and substantial economic losses, indicating the current battery fire prediction and prevention strategies need to be further improved, especially during storage and transport [5,6]. To mitigate fire hazards caused by Li-ion batteries, considerable research efforts have been devoted to this field at component-material level, cell level, and multi-battery level employing many experimental techniques. For example, the accelerating rate calorimetry (ARC) can provide an adiabatic condition to study the battery thermal runaway under controlled environmental temperature [7–15], and it can also reveal the influence of battery arrangements [12], connection modes [13], different processes [11], and environment [14,15] on thermal runaway propagation. Other techniques, such as C80 microcalorimeter [16], differential scanning

calorimetry (DSC) [17], vent sizing package 2 (VSP2) [17,18], external radiation [19,20], copper slug battery calorimeter (CSBC) [21,22] and hot oven [23–25], also have been widely adopted to test different batteries in the laboratory. Particularly, the hot oven, which has a larger internal volume and minimizes the influence of battery heat generation on the ambient temperature, is also a good choice for experimental investigation.

Most past studies focused on the thermal stability of component materials, exothermic (or self-heating) process of a single cell, or thermal runaway propagation within the battery modules. However, the self-heating characteristics of a larger quantity of batteries, such as those in storage and transportation that are not in operation and with the circuit open, are still not well understood. If heat generation from exothermic reactions exceed the environmental cooling, the self-heating ignition can be initiated [31–33]. Thus, a large battery pile could self-ignite without any operation current and even at the ambient temperature. Recently, He *et al.* [33] tested the self-ignition of open-circuit prismatic battery piles up to 4 cells with 30% SOC in the oven. They found that the critical ambient temperature for self-heating ignition decreased as the number of cells increased, which satisfied the classical self-ignition theory [31] and also verified numerically [34]. Nevertheless, Liu *et al.* [32] found the critical boundary temperature for the self-ignition of open-circuit pouch battery pile was insensitive to the number of cells, against the expected hot-plate test results. Therefore, it is important to investigate further if the classical self-ignition theory used in combustion and fire of organic fuels can apply to more complex Li-ion battery cells. Moreover, the unknown influence of battery type, SOC, size, and packing configurations on the battery self-heating ignition risk should be quantified to guide the fire-protection strategies of storing and transporting batteries. Currently, air transport requires for the SOC that should be less than 30% [35], whereas such limit does not specify the battery type or pack size. The relevant limitation is not clearly enforced in some regional regulations for road, rail, and sea transportation [36], as well as the international regulations for warehousing. Therefore, more investigations are needed to lower the fire risk and improve the relevant provisions.

In this work, the open-circuit cylindrical Li-ion battery with different pile sizes (or cell numbers) and SOCs were tested through the classical hot-oven method. The ignition phenomena, self-ignition temperature, effective kinetic parameters, and thermal properties will be discussed and analyzed in detail. Furthermore, experimental results will be upscaled to predict the self-ignition limit of larger-scale battery piles, which help assess the fire safety of Li-ion battery and mitigate the battery fire risk in storage and transport.

2. Experimental setup

2.1. Battery and apparatus

This test used the commercial 18650 cylindrical Li-ion batteries (ICR18650-22P, Samsung SDI Co., Ltd) that have been most widely used in tablet computers, electronic cigarettes, power banks, and electric vehicles. The positive electrode material of this cylindrical cell is the Lithium Nickel Manganese Cobalt Oxide (LiNiMnCoO₂ or NMC111), and the negative electrode is made of intercalation graphite. The cell has a height of 65 mm, a diameter of 18 mm, and a mass of 43.45 ± 0.05 g (Fig. 2a). Table 1 lists the physical parameters and charge-discharge characteristics of the cells.

Table 1. Physical and charge-discharge parameters of the cylindrical Li-ion battery cell.

Diameter (mm)	Height (mm)	Mass (g)	Nominal capacity (Ah)	Nominal voltage (V)	Charging cut-off voltage (V)	Discharging cut-off voltage (V)
18	65	43.45	2.05	3.6	4.15 ± 0.05	3.05 ± 0.05

The self-heating ignition experiments were conducted using a thermostatically controlled 408-L oven following the test procedures in the British Standards EN 15188:2007 [37] which is extensively adopted in bench-scale experiments to determine the self-ignition temperature (SIT) and the ignition delay time of conventional fuels. The oven used in this work can provide a constant ambient temperature up to 250 °C with

the thermal stability of ± 1 °C at 1 atm. Inside this oven, the tested battery pile was placed in a mesh cage to minimize the environmental airflow and prevent the oven damage from the extensive burning and explosion of the battery pile (Fig. 2b). Several thin K-type thermocouples with the bead diameter of 0.2 mm and the accuracy of 0.1 °C were used to monitor the ambient temperature T_a and the cell temperature T_b . The thermocouples were fixed on the center surface of each cell and within the gap between cells, so that they would not affect the contact between battery cells. A data logger was used to collect the temperature information of the oven and all battery cells. The mass for each battery cell was measured by a scale with an accuracy of 0.1 g before and after the experiment. The entire experimental process was recorded by a front-view video camera.

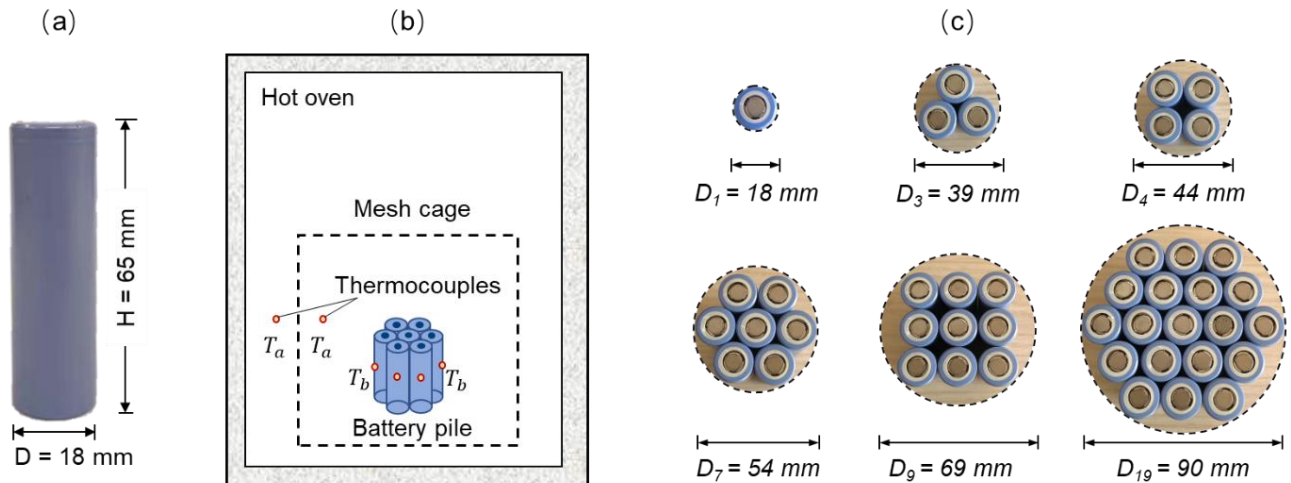


Fig. 2. (a) Photos of the experimental sample, (b) schematic of hot-oven test, and (c) photographs of the cylindrical battery piles.

2.2. Controlling parameters and procedures

In addition to the oven ambient temperature, two key battery parameters are controlled:

- (1) *Number of cells (N) or size of the pile.* The battery piles of 1, 3, 4, 7, 9, and 19 cells were tested where the open-circuit cells were horizontally stacked and fixed by thin steel wires as the cylindrical shape. Then, the equivalent diameter (D) of this cylindrical pile ranged from 18 mm (1 cell) to 90 mm (19 cells), as illustrated in Fig. 2c.
- (2) *State of Charge (SOC).* Three SOC of 30%, 80%, and 100% were selected. Most of the commercial Li-ion batteries are operated between 30% and 80% to increase the lifespan [38]. The fully charged battery (100% SOC) was also tested to consider the extreme case.

Note that the fire and explosion of 19-cell battery pile was so intense that the internal wall and door locker of the oven were severely damaged. Thus, for the self-ignition of 19 cells, only the batteries with 100% SOC were tested before the damaged oven was sent for maintenance.

Before the test, the state of charge (SOC) for each battery was calibrated. Each battery cell was fully charged by Constant Current-Constant Voltage mode, and then discharged with a constant current to the targeted SOC. Afterward, all batteries were left for at least three hours to avoid the influence of internal heating during the charging and discharging process. The oven was first preheated to the desired temperature and then stabilized for at least 10 min. Then the battery pile was carefully placed in the mesh cage, ensuring minimal contact area between the bottom surface of the battery pile and mesh cage to minimize the effect of heat conduction from the mesh cage. The expected exposure time (or induction time) in the oven is less than 2 hours. During the tests, the air inlet and outlet openings of the oven were left open to make sure that the fresh air can enter whereas the gas released from the self-heating reactions can go out.

The supercritical temperature was defined as the minimum oven ambient temperature that enabled the self-heating ignition, and the subcritical temperature was defined as the maximum ambient temperature that prevented the self-heating ignition. Experiments were conducted under different ambient temperatures until the

temperature difference between the supercritical and subcritical temperatures was within 8 °C. Then, the critical ambient temperature for the self-heating ignition T_a^* could be regarded as the average value of supercritical and subcritical temperatures. At least two repeating tests were conducted to ensure the experimental repeatability, and especially more tests were repeated near the critical conditions.

3. Results and discussion

3.1. Self-heating ignition phenomena and mass loss

Figure 3 shows a typical self-heating ignition processes of a three-cell battery pile at 80% SOC, when the oven ambient temperature (T_a) was at 165 °C. Initially, the battery is preheated by the oven to reach the ambient temperature within 20 min (Fig. 3a). During this stage, no obvious swelling phenomenon was observed, different from prismatic cells [33] and pouch cells [32], because the cylindrical metal case had better mechanical stability.



Fig. 3. Self-heating ignition phenomena of a 3-cell battery pile with 80% SOC under the oven ambient temperature of 165 °C, (a) preheating to ambient temperature, (b) electrolyte leakage, (c) gas jet, (d) safety valve fully open with an intense gas jet, (e) flame jet, and (f) intense fire.

Afterward, the battery temperature continued to increase due to internal exothermic reactions, and a small amount of electrolyte started to leak from the cathode at around 22 min (Fig. 3b). Such leakage phenomenon indicated the cracking of the battery safety vent, which could be perceived as the beginning of venting. The accumulated gases inside the battery increased the internal pressure, which further damaged the safety vent. After another 3 min, a large amount of gas and smoke started to release, shown as a gas jet (Fig. 3c). The gas jet lasted for about 15 s along, and then a loud sound was heard, which indicated that the safety valve was fully open (Fig. 3d). A flame jet was quickly piloted in a few seconds, and the strong propulsion of gas jet moved and tipped battery pile (Fig. 3e). The burning process was intense and accompanied by intense smokes and sparks, which could be the burning of Lithium metal [39] (Fig. 3f).

For the self-ignition of cell number $N \leq 4$, any battery within the pile could first go through thermal runaway, as expected. For cell number $N > 4$, thermal runaway always first occurred to the central cell inside the pile, because it had the weakest cooling condition. Once self-ignition occurred, all cells would catch the fire almost at the same time. Figure 4a compares the residue of battery piles before and after the self-ignition. After the self-heating ignition and the associated battery fire, the safety valves were broken, and the molten aluminum was re-solidified into several balls around the broken safety vent. The cells were also covered by the black char materials from the flame. Figure 4b illustrates the mass loss of the battery cell after self-ignition with different SOC levels. As expected, the mass loss of each cell increases as the SOC increases, consistent with the

observation that more smoke was released at a higher SOC. Particularly, the mass loss increases from 6.2 g (~14 %) to 15 g (~35%) as the SOC increases from 30 % to 100 %. Moreover, the mass loss seems insensitive to the pile size, which has a good agreement with previous study [32]. On the other hand, below the critical ambient temperature, no ignition occurred, and both the battery appearance and mass had the negligible change.

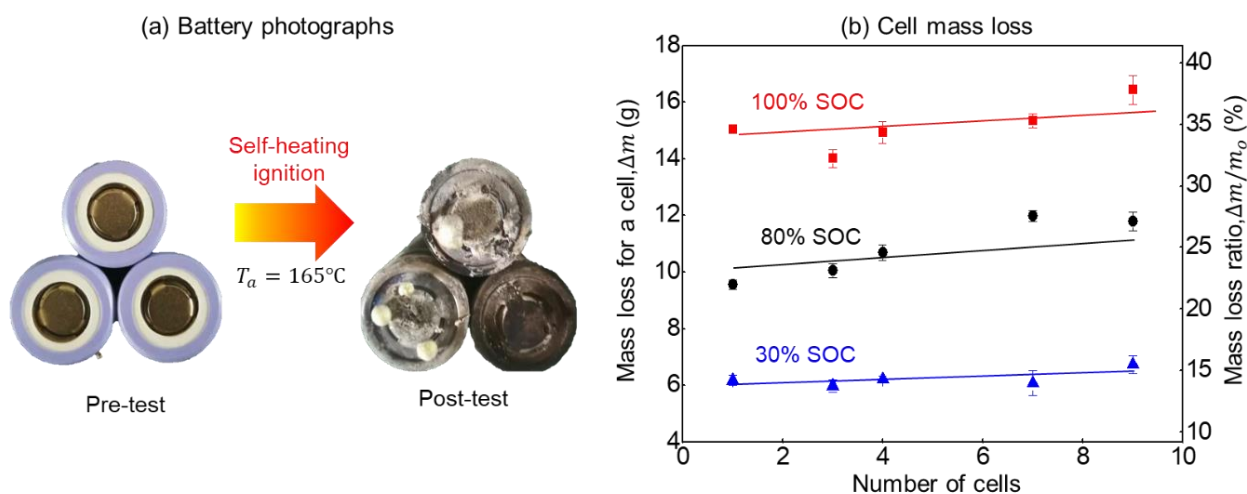


Fig. 4. (a) Photos of a 3-cell battery pile with 80% SOC before and after the experiment, and (b) mass loss and the mass-loss ratio of cells after self-heating ignition.

3.2. Temperature evolution

Figure 5a shows the typical temperature evolution during the self-ignition process of battery pile with 3 cells at the supercritical temperature of $T_a = 165^\circ\text{C}$ (the same test in Fig. 3). Based on the temperature evolution, there are three stages for self-heating ignition: (I) pre-heating, $T_b < T_a$, (II) self-heating, $T_b > T_a$, and (III) thermal runaway, $T_b \gg T_a$. During the first 20-min pre-heating period, the average heating rate of the battery was 0.1°C/s . Afterward, the battery entered the self-heating stage, where all cell temperatures exceed the oven temperature, so that the environment started to cool down the battery pile. During this stage, the exothermic reactions inside the battery dominated the temperature increase, and the initial self-heating rate was small (about 0.2°C/s). The battery temperature decreased slightly at approximately 22 min, which was caused by the failure of safety vent with gas and electrolyte leakage (see Fig. 3b). Nevertheless, the gas jet only temporarily slowed down the self-heating, which is not enough to impede the further temperature increasing. And after a short period, the battery temperature quickly raised at a heating rate of about 20°C/s , and exceeded 350°C when flame occurred (Fig. 3e, f). The intense battery fire only lasted for 2 min. After extinction, all battery cells quickly cooled down and eventually approached to the ambient temperature.

For comparison, Fig. 5b shows the failed self-ignition case at the subcritical temperature of $T_a = 156^\circ\text{C}$. There are also three noticeable stages: (I) pre-heating, $T_b < T_a$, (II) self-heating, $T_b > T_a$, and (III) thermal equilibrium, $T_b \rightarrow T_a$. The pre-heating stage was essentially like the case of self-ignition in Fig. 5a, playing an induction role for the self-heating behavior. During the self-heating stage, the battery temperature exceeded the ambient for more than 35°C . Similarly, a minor temperature fluctuation occurred at approximately 30 min due to the electrolyte leakage through the safety vent, which could be also regarded as a signal for venting. However, its self-heating rate was lower than 0.5°C/s and then gradually decreased to 0°C/s . In the cooling stage, the temperature of all battery cells continuously decreased, and finally reached the thermal equilibrium with the ambient temperature ($T_a = T_b$). The temperature evolution curves for different SOC and cell numbers have a similar trend (see Appendix).

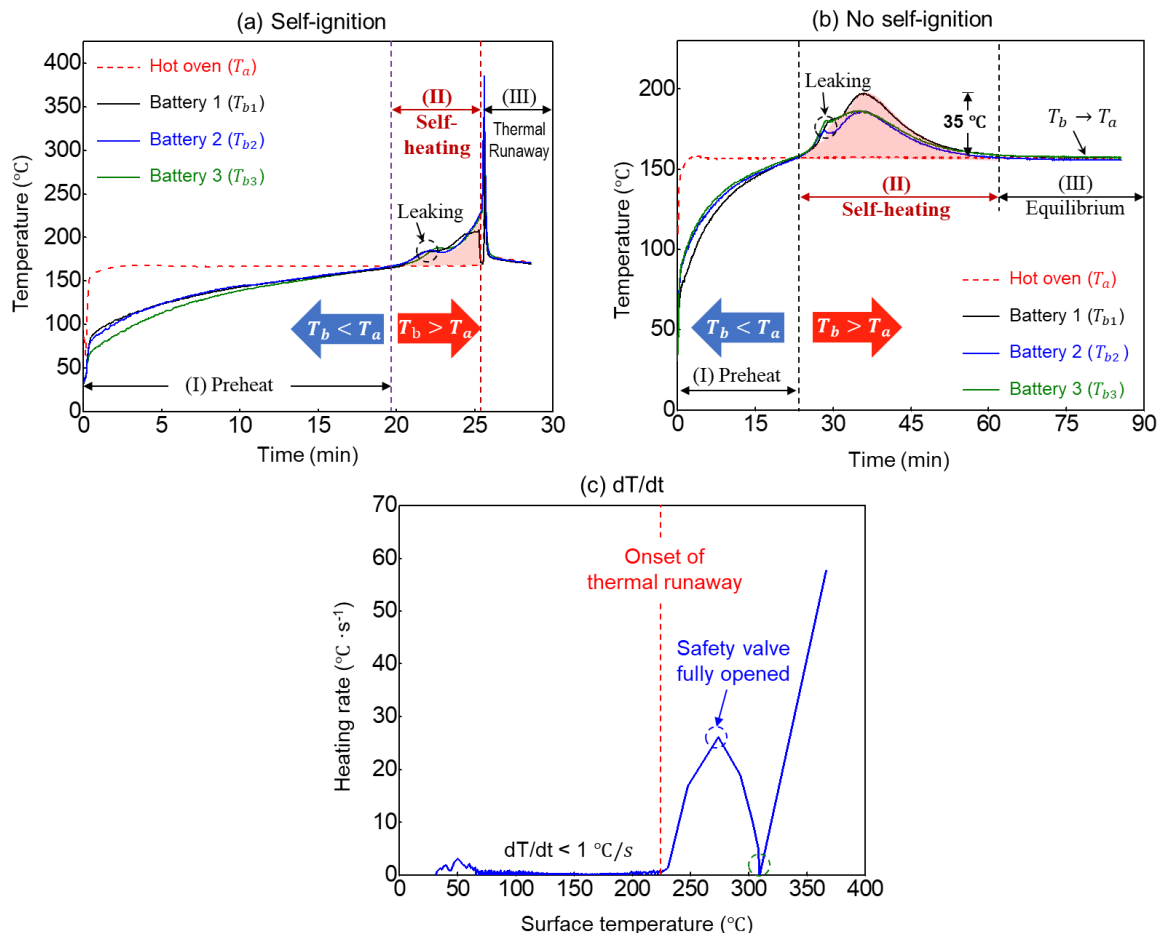


Fig. 5. The curves of temperature evolution and temperature-increasing rate for the 3-cell battery piles with 80% SOC (a, c) self-ignited at an ambient temperature of 165 °C, and (b) thermal equilibrium at 156 °C.

To explore the characteristics temperature of self-heating ignition, Fig. 5c further shows the heating rate of battery #2 in Fig. 5a as a function of surface temperature. When the surface temperature of the cell reached around 230 °C, the self-heating rate started to rise dramatically, indicating the onset of thermal runaway. There was a distinct decrease in the self-heating rate when the battery temperature exceeded 265 °C, which was the result of a fully opening of the safety valve (Fig. 3d). Afterward, when the temperature reached 310 °C, a second increase of the self-heating rate took place. It may be caused by the decomposition and oxidation of electrolyte or binder when the ambient oxygen entered [40].

3.3. Characteristic temperatures for venting and thermal runaway

Figure 6a shows the temperature when the electrolyte leakage occurred, which is a sign of battery failure. Such a leakage temperature decreases as the SOC increases, and as expected, is insensitive to the size of the battery pile. Specifically, the failure temperature for 30%, 80%, and 100% SOC are 203±3 °C, 190±3 °C, and 163±3 °C, respectively. It is because the critical decomposition temperature is lower for cells with higher SOC.

Figure 6b summarized the characteristic battery surface temperature for the onset of thermal runaway. Despite a large variation, the onset temperature decreases with increasing SOC. Specifically, the thermal runaway occurs at about 260 °C for 30% SOC and about 230 °C for 80% and 100% SOC, which agrees well with the literature value of the thermal analysis [16] and single-battery tests [9,22]. Also, the onset temperature of thermal runaway is irrelevant to the number of cells, as expected. Figure 6c shows the trend of measured peak surface temperature during the thermal runaway as a function of battery SOC and pile size. As the SOC increases, the battery fire becomes more intensive, so that the peak temperature increases. Moreover, for a pile of multiple cells, the thermal runaway starts to propagate between cells [14,15], so that the jet flame and explosion of battery also become more destructive. Then, the heating from the flame to the battery can further raise the cell temperature from below 300 °C for a single cell to 600~900 °C for a pile, posing critical fire hazard.

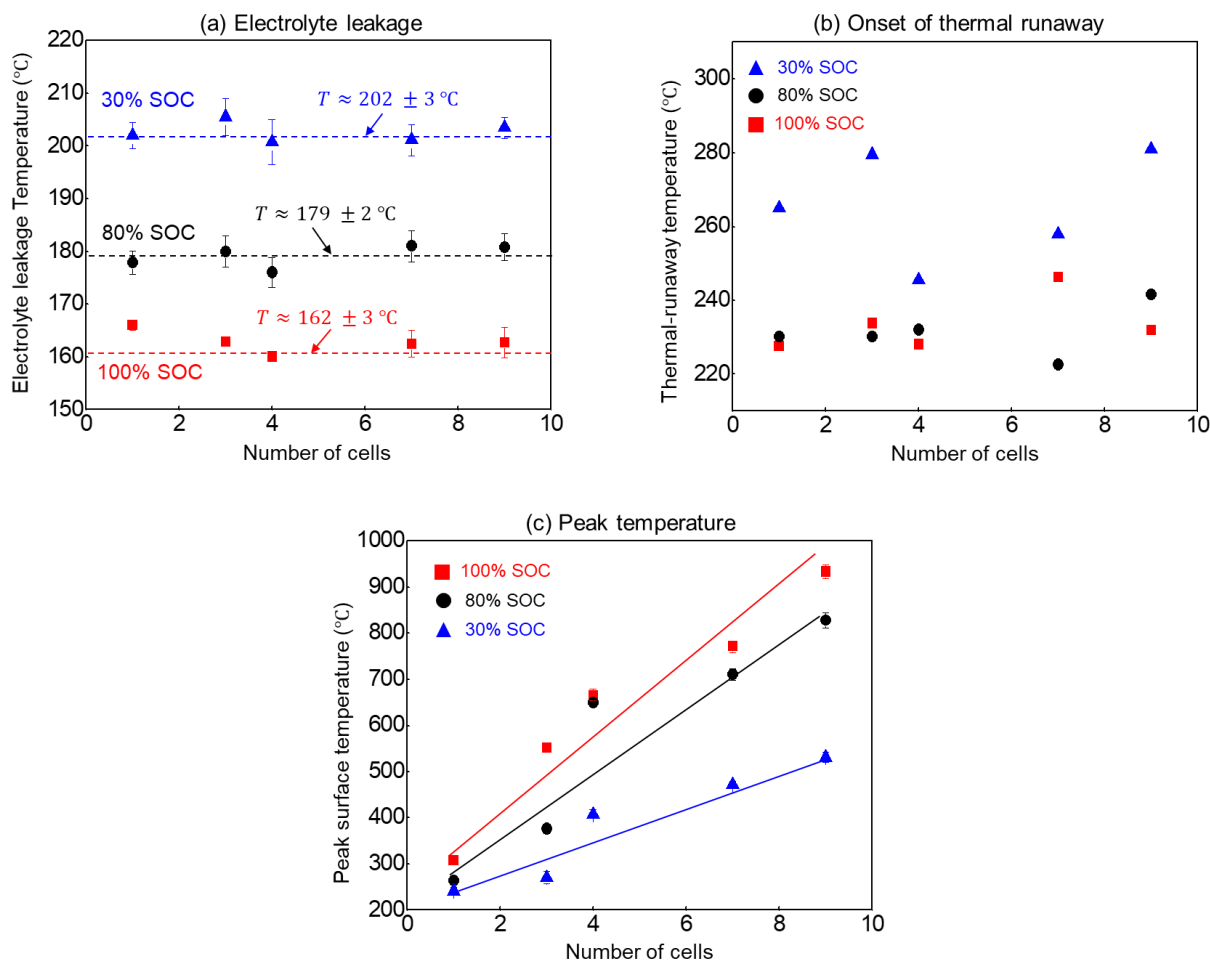


Fig. 6. (a) The cell surface temperature when the electrolyte leakage occurred, (b) the surface temperature for the onset of thermal runaway, and (c) the maximum surface temperature during the thermal runaway.

Figure 6b summarized the characteristic battery surface temperature for the onset of thermal runaway. Despite a large variation, the onset temperature decreases with increasing SOC. Specifically, the thermal runaway occurs at about 260 °C for 30% SOC and about 230 °C for 80% and 100% SOC, which agrees well with the literature value of the thermal analysis [16] and single-battery tests [9,22]. Also, the onset temperature of thermal runaway is irrelevant to the number of cells, as expected. Figure 6c shows the trend of measured peak surface temperature during the thermal runaway as a function of battery SOC and pile size. As the SOC increases, the battery fire becomes more intensive, so that the peak temperature increases. Moreover, for a pile of multiple cells, the thermal runaway starts to propagate between cells [14,15], so that the jet flame and explosion of battery also become more destructive. Then, the heating from the flame to the battery can further raise the cell temperature from below 300 °C for a single cell to 600~900 °C for a pile, posing critical fire hazard.

3.4. Critical ambient temperature for self-ignition

The critical ambient temperatures (T_a^*) to allow the self-heating ignition with different battery SOC and pile sizes from 1 cell to 19 cells are summarized in Fig. 7a. The value of T_a^* decreases as the number of cells (N) increases, agreeing with the classical self-ignition theory [31]. Specifically, for 30 % SOC, which is the maximum value for air transport [35], the critical ambient temperature for self-ignition decreases from 192 °C to 165 °C, as the pile size increases from 1 cell to 9 cells. For the fully charged battery piles (100% SOC), the critical ambient increases from 135 °C (19 cells) to 162 °C (1 cell). Therefore, both the larger pile size and the higher SOC can lead to the higher risk of self-ignition at the lower critical ambient temperature during the storage and transport.

The Frank-Kamenetskii (F-K) theory has been applied extensively in lab-scale experiments to investigate self-heating ignition limits of hydrocarbon fuels, such as coal [41], wheat biomass [42] and wood pellets [43].

It assumes a one-dimensional (1-D) heat transfer model for self-heating and the heat generation from a one-step exothermic reaction, which has also been applicable for battery cells [9]. For the subcritical cases (Fig. 5b), the surface temperatures of cells gradually cooled down to the ambient temperature and finally reached the steady-state, which also satisfied the boundary condition of F-K theory. Therefore, F-K theory could be employed in this work to analyze the characteristics of self-ignition and determine the effective kinetics and thermal properties of battery piles.

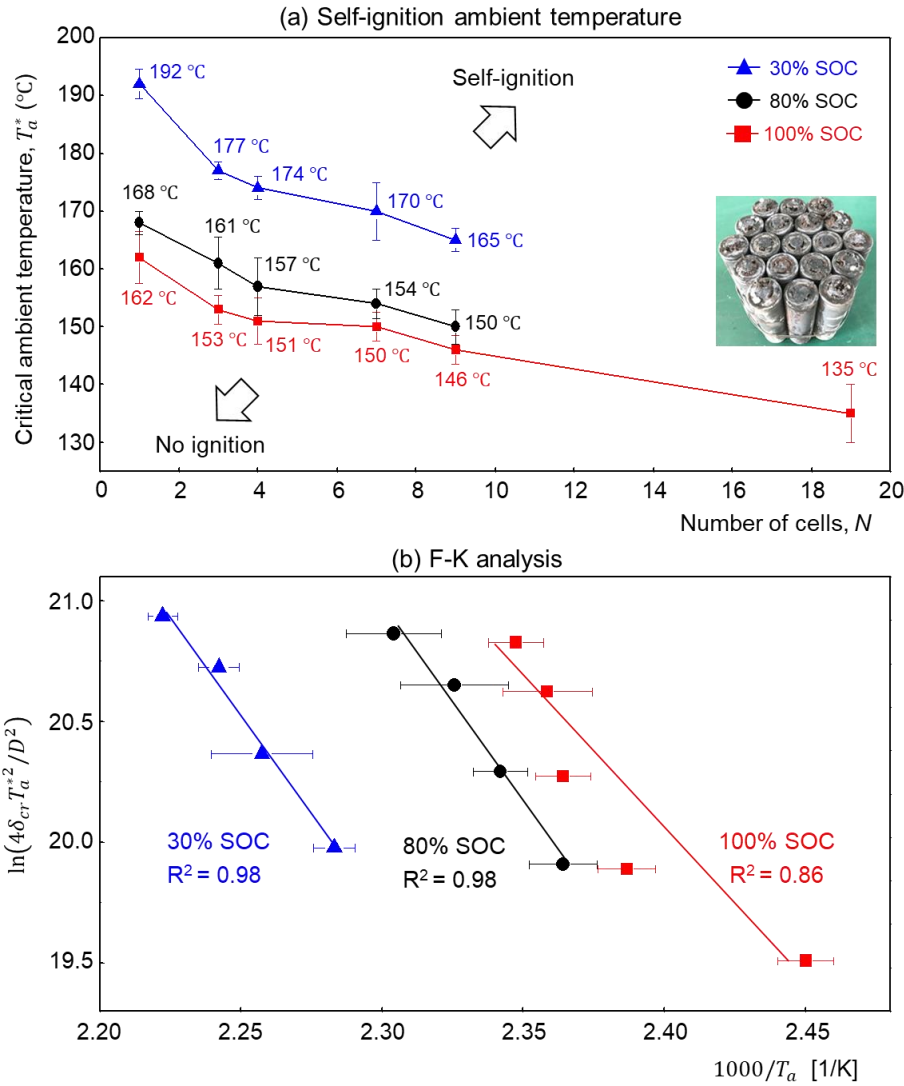


Fig. 7. (a) The critical ambient temperatures (T_a^*) varying with the battery SOC and pile size, and (b) F-K plot for cells with NCM cathode material, where a linear fit is used to extract effective battery parameters.

According to the F-K theory, a critical dimensionless number δ_{cr} could be used to quantify the possibility of self-heating ignition, which is only related to the sample geometry for the same fuel and expressed as

$$\delta_{cr} = \frac{EL^2 f \Delta H}{kRT_a^{*2}} \exp\left(-\frac{E}{RT_a^*}\right) = \frac{ED^2 f \Delta H}{4kRT_a^{*2}} \exp\left(-\frac{E}{RT_a^*}\right) \quad (1)$$

where the E is the activation energy; $L = D/2$ stands for the characteristic length; f is the mass function that depends on the concentration of fuel and oxygen at any time; ΔH is the heat of reactions; k is the thermal conductivity; R is the universal gas constant; and T_a^* in Kelvin is the critical ambient temperature for self-ignition. When the δ is higher than the critical value δ_{cr} , the heating is always larger than the cooling, and the self-heating ignition will occur. For the same battery cell under the same ambient temperature, E , f , ΔH , and k can be regarded as constant, indicating that the critical ambient temperature decreases as the characteristic length increases, which agrees with the experimental data in Fig. 7a.

As a function of the geometrical shape of fuel, the critical value δ_{cr} for a general cylinder is [31]

$$\delta_{cr} = 2.0 + 0.84 \left(\frac{D}{H} \right)^2 \quad (2)$$

where D is the equivalent diameter of the battery pile, and $H = 65$ mm is the height of the 18650 battery cell. Thus, there are two limiting values of δ_{cr}/D^2 for a single cell and an infinite number of cells as

$$\frac{\delta_{cr}}{D^2} = \frac{2.0}{D^2} + \frac{0.84}{H^2} = \begin{cases} 6389 & (N = 1, D = 18 \text{ mm}) \\ 200 & (N = \infty, D = \infty) \end{cases} \quad (3)$$

Table 2. The value of δ_{cr} for battery piles in this work, where $H = 65$ mm for the 18650 cell.

Cell No.	D (mm)	D/H	δ_{cr}	δ_{cr}/D^2
1	18.0	0.28	2.07	6389
3	38.8	0.60	2.30	1528
4	43.5	0.67	2.38	1258
7	54.0	0.83	2.58	885
9	68.9	1.06	2.94	619
19	90.0	1.38	3.60	444
36	145.3	2.24	6.21	294
100	247.1	3.80	14.13	231
∞	∞	∞	∞	200

Table 2 listed the calculated values of δ_{cr} and δ_{cr}/D^2 for battery piles of different pile size. Rearranging Eq. (1) gives

$$\ln \left(\frac{4\delta_{cr}T_a^{*2}}{D^2} \right) = -\frac{E}{R} \left(\frac{1}{T_a^*} \right) + \ln \left(\frac{E}{R} \cdot \frac{f\Delta H}{k} \right) \quad (4)$$

where the left-hand side depends on the ambient condition and the size of the battery pile; and the second term on the right only relies on the kinetics and thermophysical parameters of the battery pile. Therefore, these parameters can be determined by plotting this linear relationship between $\ln(4\delta_{cr}T_a^{*2}/D^2)$ and $1/T_a^*$, where the slope is $-E/R$, and the intercept corresponds to $\ln(Ef\Delta H/Rk)$.

The F-K plot for the self-heating ignition of the battery pile is depicted in **Fig. 7b**, which neglects the data of 1 cell data, since it is a special case. Error bars in x-direction represent the standard deviation of critical ambient temperatures extracted from experimental results, while the error bars in the y-axis are negligibly small. The values of R^2 value and thermophysical parameters of battery piles are listed in **Table 3**, where good agreements show the rationality and validity of F-K analysis application for this work. The global activation energies of battery piles are 101 ± 24 kJ/mol (100% SOC), 136 ± 14 kJ/mol (80% SOC), and 135 ± 12 kJ/mol (30% SOC), respectively.

Table 3. Linear fit and thermo-physical parameters base on F-K theory

SOC	Slope ($-E/R$)	Intercept [$\ln(Ef\Delta H/Rk)$]	R^2	k [9] (W/m-k)	E (kJ/mol)	$f\Delta H$ (W/m ³)
100%	-12.1 ± 2.9	49.1 ± 6.8	0.86	5	101 ± 24	8.7×10^{17}
80%	-16.4 ± 1.7	58.7 ± 3.9	0.98	5	136 ± 14	9.5×10^{21}
30%	-16.3 ± 1.5	57.1 ± 3.3	0.98	5	135 ± 12	1.9×10^{21}

Note that the cathode material of the battery used in this work is LiNiMnCoO_2 (NMC111) while this critical temperature for other 18650 NMC cells shall be different. According to the different molar ratios of nickel-manganese-cobalt, the types of common NMC cathode materials are NMC111, NMC 532, NMC622, and

NMC811. And the higher nickel content NMC cells have, the more thermal unstable they will be. For example, Wang et al. [44] found that the internal temperatures of NMC cells during the thermal runaway have an order of $NMC622 \geq NMC532 \geq NMC111$.

3.5. Scale-up for one-layer battery pile

The thermo-physical parameters of battery piles extracted from lab-scale tests could be used to predict the self-ignition limit of larger-scale battery piles. Here, we first predict the 18650 battery piles that are horizontally stacked into the cylindrical layer, which has a constant height of 65 mm (1 layer) and is the same as the lab-scale test. Then, the critical F-K number δ_{cr} could be calculated from Eq. (2) [31] with the equivalent diameter (D) of the pile cylinder. Based on the effective kinetic and thermal properties of the cells in Table 3, the correlation between critical ambient temperature and battery pile size in Eq. (4) could be further expressed as

$$\ln\left(\frac{4\delta_{cr}T_a^{*2}}{D^2}\right) = \ln\left(4T_a^{*2}\left(200 + \frac{2}{D^2}\right)\right) = \begin{cases} -\frac{1.21 \times 10^4}{T_a^*} + 49.1 & (100\% \text{ SOC}) \\ -\frac{1.64 \times 10^4}{T_a^*} + 58.7 & (80\% \text{ SOC}) \\ -\frac{1.63 \times 10^4}{T_a^*} + 57.1 & (30\% \text{ SOC}) \end{cases} \quad (5)$$

where the single layer of battery pile is considered ($H = 65$ mm).

The extrapolated critical ambient temperature for a larger battery pile is presented in Fig. 8a. As predicted by Eq. (3), the critical ambient temperature decreases with the increasing size. As the battery pile size exceeds 0.3 m, it essentially approaches a critical value and is only a function of SOC. Specifically, such critical value decreases from 151 °C (30% SOC) to 136°C (80% SOC), and 125 °C (100% SOC).

In other words, for the battery pack of electric vehicles, thousands of cylindrical cells are encapsulated as a single-layer battery stack with a critical size of about 2 m. If all battery cells are in the open-circuit state during assembling, transportation, and storage, the critical self-ignition temperature for this battery pack could approach to the asymptotic ambient temperature of 125-150 °C. Similarly, for the battery-based energy storage system or a shipping container, if all batteries are arranged in multiple layers, while having a gap and good cooling condition in between each layer, the required ambient temperature for self-ignition will also approach 125~150 °C. Because the normal ambient temperature rarely exceeds 60 °C, the self-ignition fire risk in a single-layer open-circuit battery pile is relatively small.

3.6. Scale-up for densely packed multi-layer battery pile

Then, let us consider a large battery pile with densely packed multiple layers of cells that are vertically stacked without any clear gap between each layer (a purely theoretical case). For simplicity, the cubic shape of battery pile with the critical F-K number $\delta_{cr} = 2.52$ [31] are applied in the calculation. With the same battery kinetic and thermophysical parameters in Table 3, the length of cubic battery pile (L) as a function of critical self-ignition ambient temperature can be expressed as

$$\ln\left(\frac{36\delta_{cr}T_a^{*2}}{L^2}\right) = \ln\left(\frac{90T_a^{*2}}{L^2}\right) = \begin{cases} -\frac{1.21 \times 10^4}{T_a^*} + 49.1 & (100\% \text{ SOC}) \\ -\frac{1.64 \times 10^4}{T_a^*} + 58.7 & (80\% \text{ SOC}) \\ -\frac{1.63 \times 10^4}{T_a^*} + 57.1 & (30\% \text{ SOC}) \end{cases} \quad (6)$$

Figure 8b shows the prediction of critical self-ignition ambient temperature for the cubic battery pile. Compared with the single-layer battery pile in Fig. 8a, the required ambient temperature for multi-layer battery pile is much lower, indicating a higher self-ignition fire risk.

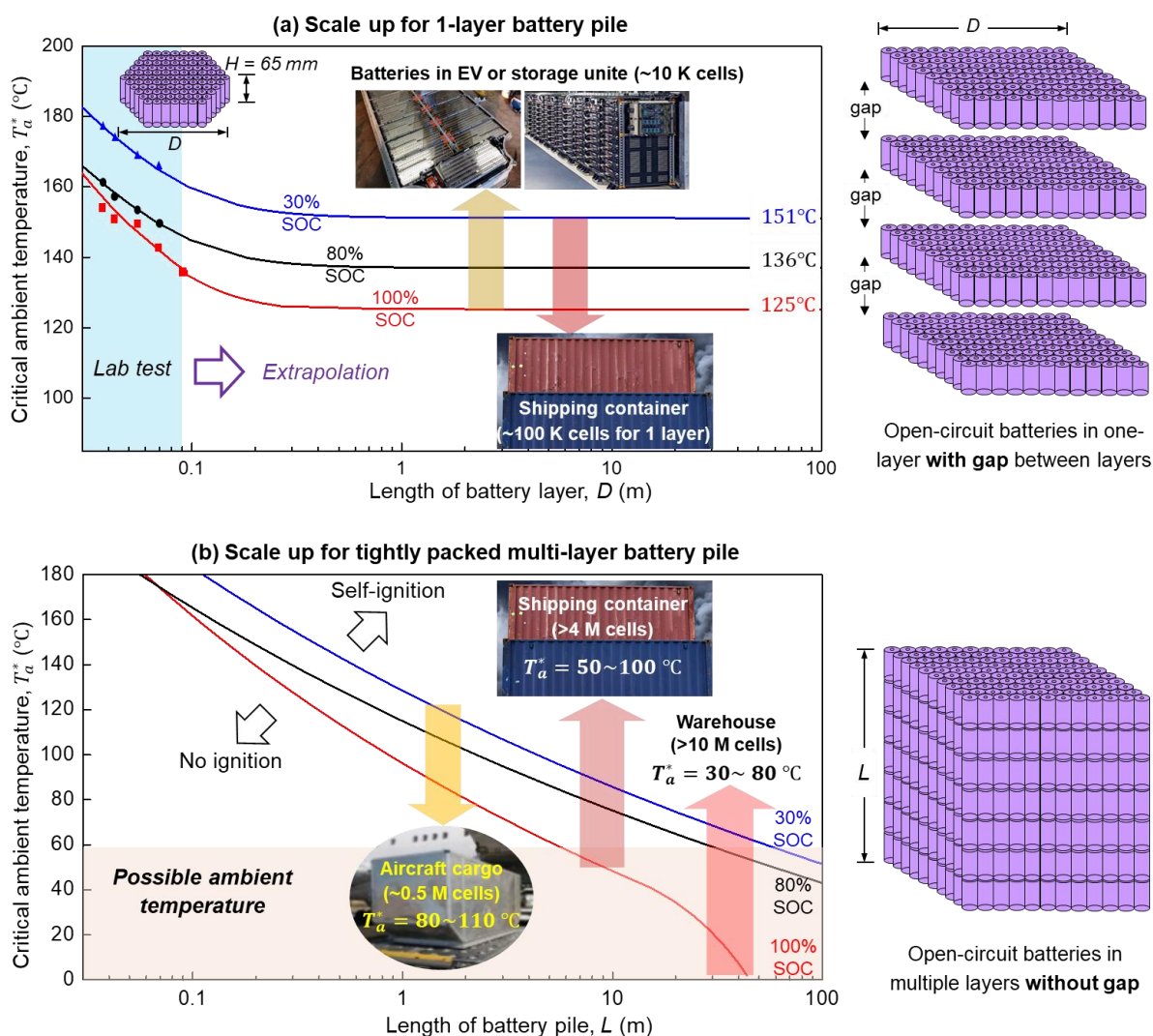


Fig. 8. Extrapolation for the critical self-ignition ambient temperature for 18650 battery piles in storage and transportation, (a) a single layer or multiple layers with gaps, and (b) densely packed with multiple layers.

In practical air-transportation scenarios, batteries could be packaged in an aircraft cargo with a dimension up to 3.2 m (length) \times 1.6 m (width) \times 2.3 m (height). More than 700 thousand cylindrical cells would be tightly fitted into this standard air cargo and roughly had a cubic shape. Then, the self-heating ignition could occur at an ambient temperature of 80-110 °C, depending on SOC. For the standard 40-foot shipping container with a dimension of 12 m (length) \times 2.3 m (width) \times 2.7 m (height), it can contain about 4 million cylindrical cells. As extrapolated in Fig. 8b, the critical ambient temperature for self-ignition could be lowered to 50-100 °C. In some extreme scenarios, such as a fire occurred near a battery warehouse where massive Li-ion batteries are stored, a shipping container exposing to direct sunshine for a few days in the tropical region, and battery storage unit next to a hot engine room, then the ambient temperature could exceed 60 °C. For the big warehouse, it could pile up even more battery cells (> 10 million). Thus, the critical ambient temperature for self-ignition could reach 30 °C, if the length of the pile is larger than 20 m.

The upscaled results in this work could still be instructive for engineers to create a safer environment for open-circuit Li-ion batteries during storage and transportation. Note that in the current experiment configuration, there is no insulation between cells, so the environmental cooling is much larger during the self-heating stage, compared to battery piles with insulation between cells. In other words, the actual self-ignition ambient temperature of commercially packed batteries could be even lower, showing a higher fire risk. Furthermore, the predicted critical ambient temperature could be lower in real scenarios. It is because (1) some battery cells have internal flaws that are more prone to thermal runaway, and (2) the low-pressure air cabin environment could reduce the natural convective cooling.

Existing international guidelines and regulations, such as UN model Regulation [4] and UN Manual of Tests and Criteria [45] are helpful to minimize this fire risk. In air transportation, except for the SOC limitation, the maximum number of batteries per package is also required based on the battery capacity [46]. For example, if the battery capacity ranges from 2.7 Wh to 100 Wh, the number of it in a package should be less than eight, which decreases the self-heating ignition risk. However, there are no international regulations for warehousing, and the enforcement gap constricts the efficiency of existing provisions [36]. Therefore, more viable investigations are needed to lower the self-heating ignition risk for real scenarios. Future experiments will study the influence of the battery type, insulation between cells (or packing method), and atmospheric pressure on the self-ignition limit. The selection of the safety factor for industrial applications and guidelines for fire protection will also be investigated as well.

4. Conclusions

In this work, the characteristics of self-heating ignition for 18650 lithium-ion battery piles in an oven are investigated with three SOC (30%, 80%, and 100%) and six sizes up to 19 cells. The ignited battery piles undergo three stages: pre-heating, self-heating, and thermal runaway, which leads to violent fire and explosion. As the SOC decreases, both the battery electrolyte leaking temperature (160~200 °C) and thermal-runaway temperature (230~280 °C) increase. The maximum battery temperature increases from 300 °C to 900 °C with increasing battery SOC and pile size.

The critical ambient temperature that allows the self-heating ignition of battery piles ranges from 135 °C to 192 °C, which decreases with SOC or battery pile size increases. The good linear fit in the Frank-Kamenetskii analysis indicates the rationality and validity of the classical self-ignition theory for battery piles. For large battery piles of multiple tightly packed layers, such as those in the shipping container and warehouse, the critical self-ignition temperature could be lower to ambient temperature (30 °C). Nevertheless, creating gaps and providing effective cooling between each battery layer could effectively lower the first risk by increasing the self-ignition ambient temperature to 125 °C for 100% SOC and 151 °C for 30% SOC. Although the current work is just a preliminary study where a purely theoretical case is presented for extrapolation, it reveals the self-ignition characteristics of open-circuit battery piles, which could provide scientific guidelines to improve battery safety and reduce fire hazards during storage and transportation.

Acknowledgments

XH would like to thank the support from HK Research Grant Council through the Early Career Scheme (25205519), Shanghai Science and Technology Committee (19160760700), and HK PolyU through the Central Research Grant (G-YBZ1). HN is supported by the Guangdong Technology Fund (2015B010118001) and National Key R&D Program of China (2018YFB0104100). The authors thank Prof. Guillermo Rein (Imperial College) for valuable discussions.

CRedit authorship contribution statement

Yanhui Liu: Data curation, Investigation, Writing - Original Draft, Formal analysis. **Peiyi Sun:** Investigation, Methodology, Writing - Review & Editing. **Shaorun Lin:** Writing - Review & Editing. **Huichang Niu:** Resources; **Xinyan Huang:** Conceptualization, Methodology, Funding acquisition, Project administration, Supervision, Writing - Review & Editing.

References

- [1] Q. Wang, B. Mao, S.I. Stolarov, J. Sun, A review of lithium ion battery failure mechanisms and fire prevention strategies, *Progress in Energy and Combustion Science*. 73 (2019) 95–131. <https://doi.org/10.1016/j.pecs.2019.03.002>.
- [2] Y.S. Duh, X. Liu, X. Jiang, C.S. Kao, L. Gong, R. Shi, Thermal kinetics on exothermic reactions of a commercial LiCoO₂ 18650 lithium-ion battery and its components used in electric vehicles: A review, *Journal of Energy Storage*. 30 (2020) 101422. <https://doi.org/10.1016/j.est.2020.101422>.
- [3] X. Feng, D. Ren, X. He, M. Ouyang, Mitigating Thermal Runaway of Lithium-Ion Batteries, *Joule*. (2020). <https://doi.org/10.1016/j.joule.2020.02.010>.
- [4] United Nations, Recommendations on the Transport of Dangerous Goods - Model Regulations (Twenty-First Revised edition), 2019. http://www.unece.org/trans/danger/publi/unrec/rev21/21files_e.html.
- [5] P. Sun, R. Bisschop, H. Niu, X. Huang, A Review of Battery Fires in Electric Vehicles, *Fire Technology*. (2020). <https://doi.org/10.1007/s10694-019-00944-3>.
- [6] Y. Liu, Q. Duan, J. Xu, H. Li, J. Sun, Q. Wang, Experimental study on a novel safety strategy of lithium-ion battery integrating fire suppression and rapid cooling, *Journal of Energy Storage*. 28 (2020) 101185. <https://doi.org/10.1016/j.est.2019.101185>.
- [7] J.S. Gnanaraj, E. Zinigrad, L. Asraf, H.E. Gottlieb, M. Sprecher, M. Schmidt, W. Geissler, D. Aurbach, A Detailed Investigation of the Thermal Reactions of LiPF₆ Solution in Organic Carbonates Using ARC and DSC, *Journal of The Electrochemical Society*. 150 (2003) A1533. <https://doi.org/10.1149/1.1617301>.
- [8] E. Zinigrad, L. Larush-Asraf, J.S. Gnanaraj, H.E. Gottlieb, M. Sprecher, D. Aurbach, Calorimetric studies of the thermal stability of electrolyte solutions based on alkyl carbonates and the effect of the contact with lithium, *Journal of Power Sources*. 146 (2005) 176–179. <https://doi.org/10.1016/j.jpowsour.2005.03.177>.
- [9] B. Mao, P. Huang, H. Chen, Q. Wang, J. Sun, Self-heating reaction and thermal runaway criticality of the lithium ion battery, *International Journal of Heat and Mass Transfer*. 149 (2020) 119178. <https://doi.org/10.1016/j.ijheatmasstransfer.2019.119178>.
- [10] C. Zhao, J. Sun, Q. Wang, Thermal runaway hazards investigation on 18650 lithium-ion battery using extended volume accelerating rate calorimeter, *Journal of Energy Storage*. 28 (2020) 101232. <https://doi.org/10.1016/j.est.2020.101232>.
- [11] X. Feng, J. Sun, M. Ouyang, F. Wang, X. He, L. Lu, H. Peng, Characterization of penetration induced thermal runaway propagation process within a large format lithium ion battery module, *Journal of Power Sources*. 275 (2015) 261–273. <https://doi.org/10.1016/j.jpowsour.2014.11.017>.
- [12] P. Huang, P. Ping, K. Li, H. Chen, Q. Wang, J. Wen, J. Sun, Experimental and modeling analysis of thermal runaway propagation over the large format energy storage battery module with Li₄Ti₅O₁₂ anode, *Applied Energy*. 183 (2016) 659–673. <https://doi.org/10.1016/j.apenergy.2016.08.160>.
- [13] J. Lamb, C.J. Orendorff, L.A.M. Steele, S.W. Spangler, Failure propagation in multi-cell lithium ion batteries, *Journal of Power Sources*. 283 (2015) 517–523. <https://doi.org/10.1016/j.jpowsour.2014.10.081>.
- [14] A.O. Said, C. Lee, S.I. Stolarov, A.W. Marshall, Comprehensive analysis of dynamics and hazards associated with cascading failure in 18650 lithium ion cell arrays, *Applied Energy*. 248 (2019) 415–428. <https://doi.org/10.1016/j.apenergy.2019.04.141>.
- [15] H. Niu, C. Chen, D. Ji, L. Li, Z. Li, Y. Liu, X. Huang, Thermal-Runaway Propagation over a Linear Cylindrical Battery Module, *Fire Technology*. (2020). <https://doi.org/10.1007/s10694-020-00976-0>.
- [16] P. Ping, Q. Wang, P. Huang, J. Sun, C. Chen, Thermal behaviour analysis of lithium-ion battery at elevated temperature using deconvolution method, *Applied Energy*. 129 (2014) 261–273. <https://doi.org/10.1016/j.apenergy.2014.04.092>.
- [17] C.Y. Wen, C.Y. Jhu, Y.W. Wang, C.C. Chiang, C.M. Shu, Thermal runaway features of 18650 lithium-ion batteries for LiFePO₄ cathode material by DSC and VSP2, *Journal of Thermal Analysis and Calorimetry*. 109 (2012) 1297–1302. <https://doi.org/10.1007/s10973-012-2573-2>.
- [18] W.C. Chen, J. De Li, C.M. Shu, Y.W. Wang, Effects of thermal hazard on 18650 lithium-ion battery

- under different states of charge, *Journal of Thermal Analysis and Calorimetry*. 121 (2015) 525–531. <https://doi.org/10.1007/s10973-015-4672-3>.
- [19] Y. Fu, S. Lu, K. Li, C. Liu, X. Cheng, H. Zhang, An experimental study on burning behaviors of 18650 lithium ion batteries using a cone calorimeter, *Journal of Power Sources*. 273 (2015) 216–222. <https://doi.org/10.1016/j.jpowsour.2014.09.039>.
- [20] P. Ping, Q.S. Wang, P.F. Huang, K. Li, J.H. Sun, D.P. Kong, C.H. Chen, Study of the fire behavior of high-energy lithium-ion batteries with full-scale burning test, *Journal of Power Sources*. 285 (2015) 80–89. <https://doi.org/10.1016/j.jpowsour.2015.03.035>.
- [21] X. Liu, S.I. Stolarov, M. Denlinger, A. Masias, K. Snyder, Comprehensive calorimetry of the thermally-induced failure of a lithium ion battery, *Journal of Power Sources*. 280 (2015) 516–525. <https://doi.org/10.1016/j.jpowsour.2015.01.125>.
- [22] X. Liu, Z. Wu, S.I. Stolarov, M. Denlinger, A. Masias, K. Snyder, Heat release during thermally-induced failure of a lithium ion battery: Impact of cathode composition, *Fire Safety Journal*. 85 (2016) 10–22. <https://doi.org/10.1016/j.firesaf.2016.08.001>.
- [23] J. Jiang, H. Fortier, J.N. Reimers, J.R. Dahn, Thermal Stability of 18650 Size Li-Ion Cells Containing LiBOB Electrolyte Salt, *Journal of The Electrochemical Society*. 151 (2004) A609. <https://doi.org/10.1149/1.1667520>.
- [24] P.J. Bugryniec, J.N. Davidson, D.J. Cumming, S.F. Brown, Pursuing safer batteries: Thermal abuse of LiFePO₄ cells, *Journal of Power Sources*. 414 (2019) 557–568. <https://doi.org/10.1016/j.jpowsour.2019.01.013>.
- [25] T.D. Hatchard, D.D. MacNeil, A. Basu, J.R. Dahn, Thermal Model of Cylindrical and Prismatic Lithium-Ion Cells, *Journal of The Electrochemical Society*. 148 (2001) A755. <https://doi.org/10.1149/1.1377592>.
- [26] C. DREW, J.A.D. MOUAWAD, Safety Board Reports New Details on Battery Fire, *New York Times*. (2013). <https://cn.nytimes.com/business/20130309/c09boeing/en-us/> (accessed February 27, 2020).
- [27] C. Toczaer, Cargo pallet catches fire at HKG, cause uncertain, *Air Cargo World*. (2019). <https://aircargoworld.com/news/stakeholders/airports/cargo-pallet-catches-fire-at-hkg-cause-uncertain/> (accessed February 27, 2020).
- [28] Fire breaks out at battery warehouse in Lyon, *One News Page VIDEO*. (2019). <https://www.onenewspage.com/video/20191008/12346829/Fire-breaks-out-at-battery-warehouse-in-Lyon.htm> (accessed February 27, 2020).
- [29] safety4sea, Lithium batteries caused the fire onboard Cosco Pacific - SAFETY4SEA, (2020). <https://safety4sea.com/lithium-batteries-caused-the-fire-onboard-cosco-pacific/> (accessed February 27, 2020).
- [30] CHRISTIAN FERNSBY, Lithium batteries cause of fire on Cosco Pacific ship, *Post Online Media*. (2020). <https://www.poandpo.com/news/lithium-batteries-cause-of-fire-on-cosco-pacific-ship-812020331/> (accessed August 15, 2020).
- [31] V. Babrauskas, *Ignition handbook: principles and applications to fire safety engineering, fire investigation, risk management and forensic science*, Fire Science Publishers, 2003.
- [32] Y. Liu, P. Sun, H. Niu, X. Huang, G. Rein, Propensity to self-heating ignition of open-circuit pouch lithium-ion battery pile on a hot boundary, *Fire Safety Journal*. (2020). <https://doi.org/10.1016/j.firesaf.2020.103081>.
- [33] X. He, F. Restuccia, Y. Zhang, Z. Hu, X. Huang, J. Fang, G. Rein, Experimental study of self-heating ignition of lithium-ion batteries during storage and transport: effect of the number of cells, *Fire Technology*. (2020) 1–21. <https://doi.org/10.1007/s10694-020-01011-y>.
- [34] Z. Hu, F. Restuccia, X. He, G. Rein, Numerical study of self-heating ignition of a box of lithium ion batteries during storage, *Fire Technology*. (2020). <https://doi.org/10.1007/s10694-020-00998-8>.
- [35] Federal Aviation Administration, New International Civil Aviation Organization (ICAO) Regulatory Requirements for Shipping and Transporting Lithium Batteries, 2016. https://www.faa.gov/hazmat/resources/lithium_batteries/media/SAFO16004.pdf.
- [36] H. Huo, Y. Xing, M. Pecht, B.J. Züger, N. Khare, A. Vezzini, Safety requirements for transportation of lithium batteries, *Energies*. 10 (2017) 793. <https://doi.org/10.3390/en10060793>.

- [37] European Committee for Standardization, Determination of the spontaneous ignition behaviour of dust accumulations, BS-EN 15188:2007. (2007).
- [38] Battery University, BU-415: How to Charge and When to Charge?, (2017). https://batteryuniversity.com/learn/article/how_to_charge_when_to_charge_table.
- [39] M. Schiemann, J. Bergthorson, P. Fischer, V. Scherer, D. Taroata, G. Schmid, A review on lithium combustion, *Applied Energy*. 162 (2016) 948–965. <https://doi.org/10.1016/j.apenergy.2015.10.172>.
- [40] Q. Wang, L. Jiang, Y. Yu, J. Sun, Progress of enhancing the safety of lithium ion battery from the electrolyte aspect, *Nano Energy*. 55 (2019) 93–114. <https://doi.org/10.1016/j.nanoen.2018.10.035>.
- [41] D. Wu, X. Huang, F. Norman, F. Verplaetsen, J. Berghmans, E. Van Den Bulck, Experimental investigation on the self-ignition behaviour of coal dust accumulations in oxy-fuel combustion system, *Fuel*. 160 (2015) 245–254. <https://doi.org/10.1016/j.fuel.2015.07.050>.
- [42] F. Restuccia, N. Fernandez-Anez, G. Rein, Experimental measurement of particle size effects on the self-heating ignition of biomass piles: Homogeneous samples of dust and pellets, *Fuel*. 256 (2019) 115838. <https://doi.org/10.1016/j.fuel.2019.115838>.
- [43] W. Guo, X. Bi, C.J. Lim, S. Sokhansanj, Investigation of wood pellets self-heating kinetics and thermal runaway phenomena using lab scale experiments, *Canadian Journal of Chemical Engineering*. 98 (2020) 127–137. <https://doi.org/10.1002/cjce.23592>.
- [44] H. Wang, Z. Du, X. Rui, S. Wang, C. Jin, L. He, F. Zhang, Q. Wang, X. Feng, A comparative analysis on thermal runaway behavior of Li (NixCoyMnz) O2 battery with different nickel contents at cell and module level, *Journal of Hazardous Materials*. 393 (2020) 122361. <https://doi.org/10.1016/j.jhazmat.2020.122361>.
- [45] United Nations, Manual of tests and criteria: version 7, 2019. <https://www.unece.org/index.php?id=53091&L=0>.
- [46] International Air Transport Association, Lithium Battery Guidance Document: Transport of Lithium Metal and Lithium Ion Battery, 2020. <https://www.iata.org/contentassets/05e6d8742b0047259bf3a700bc9d42b9/lithium-battery-guidance-document-2020.pdf>.

Appendix

Figure A1 compares the temperature evolution curves of the 3-cell battery pile with 100% SOC (a) self-ignited at an ambient temperature of 155 °C, and (b) thermal equilibrium at 150 °C. Figure A2 compares the temperature evolution curves of the 3-cell battery pile with 30% SOC. Figure A3 compares the temperature evolution curves of the 19-cell battery pile with 100% SOC. Figure A4 is the photos of the hot oven.

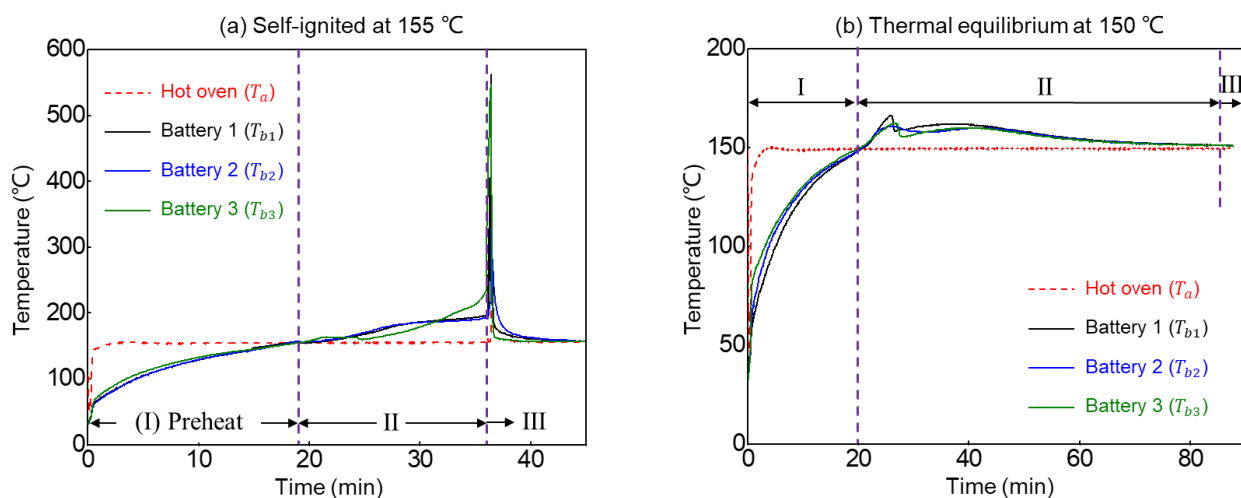


Fig. A1. The temperature evolution curves of the 3-cell battery piles with 100% SOC (a) self-ignited at an ambient temperature of 155 °C, and (b) thermal equilibrium at 150 °C.

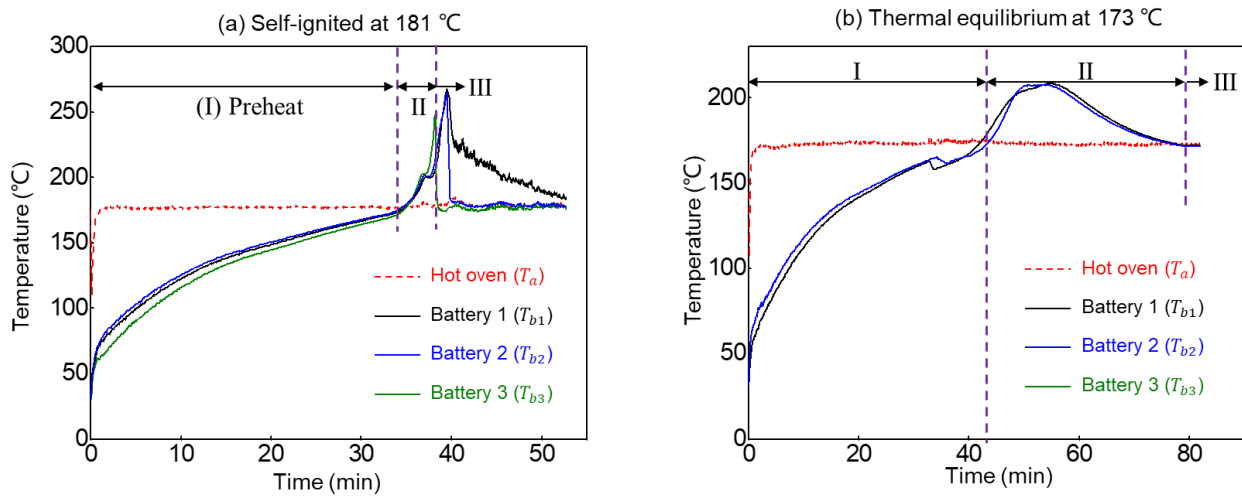


Fig. A2. The temperature evolution curves of the 3-cell battery piles with 30% SOC (a) self-ignited at an ambient temperature of 181 °C, and (b) thermal equilibrium at 173 °C.

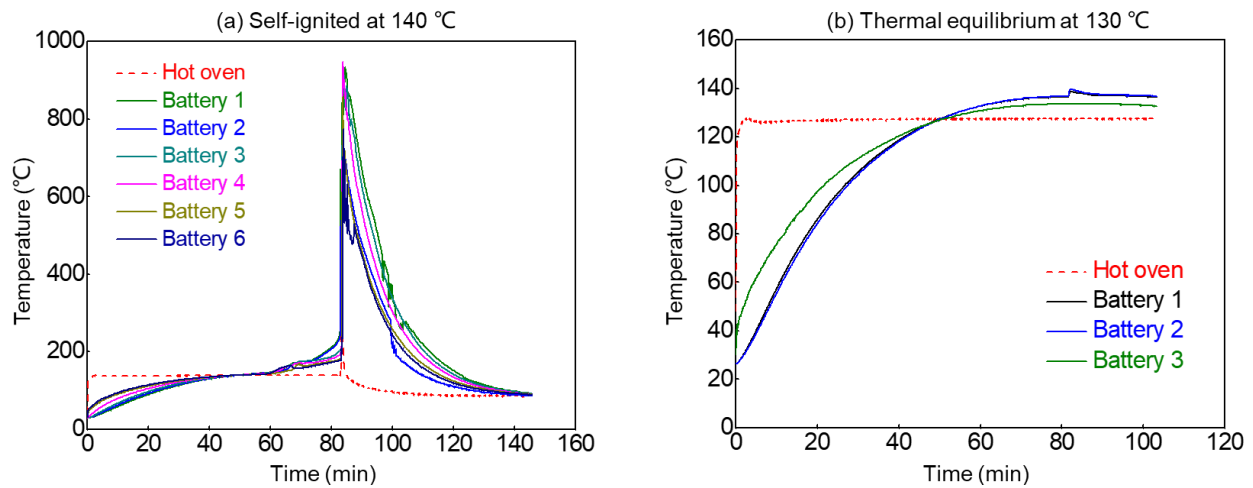


Fig A3. The temperature evolution curves of the 19-cell battery piles with 100% SOC (a) self-ignited at an ambient temperature of 140 °C, and (b) thermal equilibrium at 130 °C.



Fig A4. The photographs of the (a) external of the oven, and (b) internal of oven.